A 14-Electron Ruthenium(II) Hydride, $[RuH(CO)(P^tBu_2Me)_2]BAr'_4$ (Ar′ = 3,5-$(C_6H_3)(CF_3)_2$): Synthesis, Structure, and Reactivity toward Alkenes and Oxygen Ligands

Dejian Huang,† John C. Bollinger,† W. E. Streib,† Kirsten Folting,† Victor Young, Jr.,§ Odile Eisenstein,‡ and Kenneth G. Caulton*,†

Department of Chemistry and Molecular Structure Center, Indiana University, Bloomington, Indiana 47405, LSDSMS (UMR 5636), Université de Montpellier 2, 34095 Montpellier Cedex 05, France, and Department of Chemistry, University of Minnesota, Minneapolis, Minnesota 55455

Received December 17, 1999

Triflate in $RuH(OTf)(CO)L_2$ (L = P^tBu_2Me) can be abstracted by $NaBAr'_4$ (Ar′ = $C_6H_3(CF_3)_2$) in C_6H_5F to give 14-electron $RuH(CO)L_2^+$, which has agostic donation by one ^{t}Bu methyl group from each phosphine. This cation binds CH_2Cl_2 in an η^2 fashion, and it binds OEt_2 and H_2O in the site trans to CO. It binds ethylene trans to hydride, and additional ethylene is catalytically dimerized to *cis*- and *trans*-but-2-ene at −30 °C in C_6H_5F/toluene; this dimerization is slower in CH_2Cl_2 solvent. Propylene and H_2C═CHF also bind to $RuH(CO)L_2^+$ trans to hydride, and the latter is converted to ethylene and Ru/F products. Vinyl ethers seem to bind η^1 via ether oxygen more than η^2 via the CC bond, and trans to CO, and this species then isomerizes to the $RuL_2(CO)(\eta^2$-$CH_2CH_2OR)$ insertion product at −60 °C. In contrast, 2,3-dihydrofuran gives a cyclic oxygen-stabilized carbene complex. A discussion of the results based on DFT (B3PW91) calculations is presented in the following paper.

Introduction

We have shown earlier[1] that $RuHClL_2$ (L = P^iPr_3), a fragment available from the dimer $(RuHClL_2)_2$ present in hydrocarbon solvents, spontaneously isomerizes donor-substituted olefins to carbene ligands (eq 1).

$$RuHClL_2 + \underset{E = \text{alkoxide, amide}}{H_2C{=}CH(E)} \rightarrow L_2ClHRu{=}C(E)(CH_3) \quad (1)$$

These reactions are thermodynamically favorable in part because Ru(II) in a ligand environment devoid of π-acid ligands is a good π-donor, and the carbene is a stronger π-acid than the alternative olefin ligand. Essential to a *mechanism* for reaching this equilibrium position is the fact that the olefin reagent can coordinate cis to hydride, where it can insert into the Ru−H bond

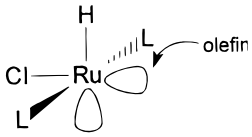

and isomerize to the hydrido carbene.[2] The 14-electron configuration of $RuHClL_2$ is thus important in achieving an empty orbital cis to hydride, which is not true of many 16-electron species $MHClL_3$;[3−9] there, the LUMO is trans to hydride.

We investigate here the influence of changing chloride to the π-acid ligand CO. We first describe the synthesis and characterization of the necessary $RuH(CO)L'_2^+$ (L′ = P^tBu_2Me).[10] The change from P^iPr_3 to P^tBu_2Me

* Corresponding author. E-mail: caulton@indiana.edu.
† Indiana University.
‡ Université de Montpellier 2.
§ University of Minnesota.

(1) Coalter, J. N., III; Spivak, G. J.; Gérard, H.; Clot, E.; Davidson, E. R.; Eisenstein, O.; Caulton, K. G. *J. Am. Chem. Soc* **1998**, *120*, 9388.
(2) Coalter, J. N., III; Bollinger, J. C.; Huffman, J. C.; Werner-Zwanziger, U.; Caulton, K. G.; Davidson, E. R.; Gérard, H.; Clot, E.; Eisenstein, O. *New J. Chem.* **2000**, *24*, 9.
(3) Hill, A. F. In *Comprehensive Organometallic Chemistry II, Vol. 7*; Abel, E. W., Stone, F. G. A., Wilkinson, G., Ed.; Pergamon: New York, 1995; p 299.
(4) (a) Poulton, J. T.; Sigalas, M. P.; Eisenstein, O.; Caulton, K. G. *Inorg. Chem.* **1993**, *32*, 5490. (b) Poulton, J. T.; Folting, K.; Streib, W. E.; Caulton, K. G.; *Inorg. Chem.* **1992**, *31*, 3190. (c) Gusev, D. G.; Vymenits, A. B.; Bakhmutov, V. I. *Inorg. Chem.* **1992**, *31*, 2. (d) Gusev, D. G.; Kuhlman, R. L.; Renkema, K. B.; Eisenstein, O.; Caulton, K. G. *Inorg. Chem.* **1996**, *35*, 6775. (e), Roper, W. R.; Wright, L. J. *J. Organomet. Chem.* **1977**, *142*, C1.
(5) (a) Maddock, S. M.; Rickard, C. E. F.; Roper, W. R.; Wright, L. J. *Organometallics* **1996**, *15*, 1793. (b) Esteruelas, M. A.; Oro, L. A.; Valero, C. *Organometallics* **1995**, *14*, 3596. (c) Esteruelas, M. A.; Lahoz, F. J.; Oñate, E.; Oro, L. A.; Zeier, B. *Organometallics* **1994**, *13*, 4258. (d) Esteruelas, M. A.; Oro, L. A.; Ruiz, N. *Organometallics* **1994**, *13*, 1507. (e) Bakhmutov, V. I.; Bertrán, J.; Esteruelas, M. A.; Lledós, A.; Maseras, F.; Modrego, J.; Oro, L. A.; Sola, E. *Chem. Eur. J.* **1996**, *2*, 815.
(6) (a) Heyn, R. H.; Macgregor, S. A.; Nadasdi, T. T.; Ogasawara, M.; Eisenstein, O.; Caulton, K. G. *Inorg. Chim. Acta* **1997**, *259*, 5. (b) Gusev, D. G.; Nadasdi, T. T.; Caulton, K. G. *Inorg. Chem.* **1996**, *35*, 6772. (c) Ogasawara, M.; Macgregor, S. A.; Streib, W. E.; Folting, K.; Eisenstein, O.; Caulton, K. G. *J. Am. Chem. Soc.* **1996**, *118*, 10189. (d) Heyn, R. H.; Caulton, K. G. *New J. Chem.* **1993**, *17*, 797. (e) Esteruelas, M. A.; Liu, F.; Oñate, E. Sola, E.; Zeier, B. *Organometallics* **1997**, *16*, 2919. (f) Esteruelas, M. A.; Lahoz, F. J.; Oñate, E.; Oro, L. A.; Sola, E. *J. Am. Chem. Soc.* **1996**, *118*, 89.
(7) (a) Hoffman, P. R.; Caulton, K. G. *J. Am. Chem. Soc.* **1975**, *97*, 4221. (b) Jung, C. W.; Garrou, P.E.; Hoffman, P. R.; Caulton, K. G. *Inorg. Chem.* **1984**, *23*, 726.
(8) Caulton, K. G. *New J. Chem.* **1994**, *18*, 25.
(9) (a) Esteruelas, M. A.; Oro, L. A.; Valero, C. *Organometallics*, **1991**, *10*, 462. (b) Sanchez Delgado, R. A.; Rosales, M.; Esteruelas, M. A.; Oro, L. A. *J. Mol. Catal. A-Chem.* **1995**, *96*, 231, and references therein.

10.1021/om9910017 CCC: $19.00
Publication on Web 05/06/2000

Scheme 1[a]

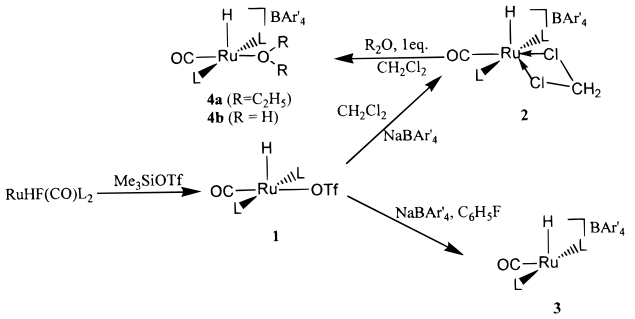

[a] L = P^{t}Bu$_2$Me.

appears to be necessitated by the fact that, in the absence of a π-donor chloride to make metastable a 14-electron configuration, agostic interactions are a viable substitute. Agostic donation by P^{t}Bu$_2$Me is apparently more potent than by P^{i}Pr$_3$. After full characterization of RuH(CO)L′$_2^+$, its reactions with the unconventional donors CH_2Cl_2, Et_2O, and H_2O are reported, followed by reactivity with olefins without, then with donor substituents E. It will appear that RuHCl(L)$_2$ and RuH(CO)(L)$_2^+$ have noticeably different reactivity with olefins. The following paper will use DFT calculations to interpret these differences.

Results

Preparation and Structure of RuH(OTf)(CO)L$_2$, 1. Reaction of RuHF(CO)L$_2$ (L = P^{t}Bu$_2$Me) with 1 equiv of Me_3SiOTf gives quantitatively RuH(OTf)(CO)L$_2$, **1**, and Me_3SiF in methylene chloride, benzene, or diethyl ether (Scheme 1).[11] Taking advantage of the strong Si−F bond (BDE = 159 kcal·mol^{-1}),[12] the exothermic reaction is complete within the time of mixing at room temperature. Although metathesis of AgOTf with metal halide is a common protocol in the synthesis of transition metal triflate complexes, it is not a productive method in this case. Instead, when RuHCl(CO)L$_2$ was treated with AgOTf in CH_2Cl_2 or in benzene, the Ag(I) mainly reacts with phosphine ligand to give [AgL$_2$][OTf].[13] The ^{1}H NMR spectrum of **1** shows a triplet at −25.4 ppm for the hydride, consistent with the hydride trans to the vacant site.[2,14] Two ^{t}Bu triplets indicate mutually trans phosphine ligands with diastereotopic ^{t}Bu groups. The CO stretching frequency of **1** appears at 1923 cm^{-1} and is much higher than that of RuHF(CO)L$_2$ (1896 cm^{-1}),[15] in agreement with weaker donation from the OTf$^-$ to the metal center.[16] Since the OTf could coordinate in a bidentate fashion and make the Ru center saturated,[17]

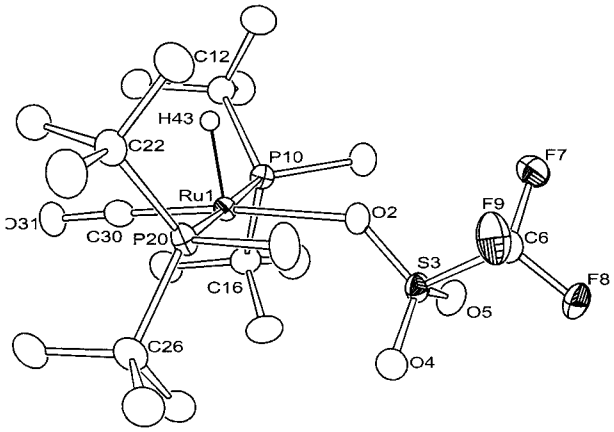

Figure 1. ORTEP diagram of RuH(OTf)(CO)(P^{t}Bu$_2$Me)$_2$; hydrogens are omitted except the one bound to Ru. Selected bond lengths (Å): Ru1−O2: 2.2088(19), Ru1−C30: 1.803(3), Ru1P10: 2.394(12), Ru1−P20: 2.3982(13), S3−O2: 1.4723(11), S3−O4: 1.4302(27). Angles (°): P20−Ru1−P10: 176.95(3), Ru1−P20−C26: 112.17(16), Ru1−P20−C22: 115.17(15), Ru1−P10−C16: 108.81(14), Ru1−P10−C12: 117.58(11), C30−Ru1−O2: 173.46(9).

X-ray crystal structure analysis of this complex was carried out. X-ray quality crystals were grown from a diethyl ether solution at −20 °C. In accord with the ^{1}H NMR spectrum, RuH(OTf)(CO)L$_2$ adopts a square-based pyramidal geometry with the hydride located at the apical site trans to the empty site (Figure 1). The OTf ligand is monodentate (the shortest distance of Ru to nonbonded oxygens of triflate is 3.795 Å), so the Ru is unsaturated. The correctness of the hydride position on that side of the RuP$_2$OC plane is supported by the fact that no ^{t}Bu methyls are directed toward it, which is different from the ^{t}Bu conformation on the other side of that plane. The shortest distance from Ru to carbon on a phosphine ligand is 3.30 Å, which is too long for an agostic interaction. The Ru−O distance (2.2088(19) Å) is much longer than that of the σ-bound ruthenium sulfonate complex, *cis*,*trans*-Ru(OSO$_2$-*p*-Tol)$_2$(H$_2$O)(CO)(PPh$_3$)$_2$ (2.165(5) and 2.162(6) Å),[18] but comparable to that of Ru−OTf (2.221(3) and 2.233(3) Å) in Ru(OTf)$_2$(CO)(Cyttp) (Cyttp = PhP(CH$_2$CH$_2$CH$_2$PCy$_2$)$_2$).[19] The long Ru−O distance is consistent with low nucleophilicity of the OTf ligand.

Synthesis and Structure of [RuH(CO)L$_2$]BAr′$_4$ and its CH_2Cl_2 Adduct. The weak coordination of OTf is in agreement with the fact that salt metathesis of **1** with 1 equiv of NaBAr′$_4$ (Ar′ = 3,5-C$_6$H$_3$(CF$_3$)$_2$) in CH_2Cl_2 at room temperature gives [RuH(CO)(η^2-CH$_2$Cl$_2$)L$_2$][BAr′$_4$], **2**, cleanly in 5 min (Scheme 1). The similar salt metathesis does not happen between RuHF(CO)L$_2$ (or RuHCl(CO)L$_2$) and NaBAr′$_4$ under the same conditions. Addition of NaBAr′$_4$ to RuHF(CO)L$_2$, or RuHCl(CO)L$_2$, in CD_2Cl_2 only broadens the hydride and the phosphine resonance peaks, indicating some interactions, presumably between Na^+ and the halides. In contrast, removal of fluoride or chloride from iridium complexes IrH$_2$F(P^{t}Bu$_2$Ph)$_2$ and IrH$_2$Cl(P^{t}Bu$_2$Ph)$_2$ by NaBAr′$_4$ is successful.[14] The reaction is also highly solvent dependent.

(10) Preliminary communication: Huang, D.; Huffman, J. C.; Bollinger, J. C.; Eisenstein, O.; Caulton , K. G. *J. Am. Chem. Soc.* **1997**, *119*, 7398. Huang, D.; Gérard, H.; Clot, E.; Young, V., Jr.; Streib, W. E.; Eisenstein, O.; Caulton, K. G. *Organometallics* **1999**, *18*, 5441.

(11) Doherty, N. M.; Critchlow, S. C. *J Am. Chem. Soc.* **1987**, *109*, 7906. Hoffman, N. W.; Prokopuk, N.; Robbins, M. J.; Jones, C. M.; Doherty, N. M. *Inorg. Chem.* **1991**, *30*, 4177.

(12) Patai, S., Rappoport, Z., Eds. In *Chemistry of Organic Silicon Compounds*; John Wiley & Sons: New York, 1989; Part I, p 385.

(13) Ogasawara, M. Personal communication.

(14) Cooper, A. C.; Clot, E.; Huffman, J. C.; Streib, W. E.; Maseras, F.; Eisenstein, O.; Caulton, K. G. *J. Am. Chem. Soc.* **1999**, *121*, 97.

(15) Poulton J. T.; Sigalas, M. P.; Eisenstein, O. Caulton, K. G. *Inorg. Chem.* **1993**, *32*, 5490.

(16) Lawrance, G. A. *Chem. Rev.* **1986**, *86*, 17.

(17) Gudat, D.; Schrott, M.; Bajorat, V.; Nieger, M.; Kotila, S.; Fleischer, R.; Stalke, D. *Chem. Ber.* **1996**, *129*, 337.

(18) Harding, P. A.; Robinson, S. D.; Henrick, K. *J. Chem. Soc., Dalton Trans.* **1988**, 415.

(19) Blosser, P. W.; Gallucci, J. C.; Wojcicki, A. *Inorg. Chem.* **1992**, *31*, 2376.

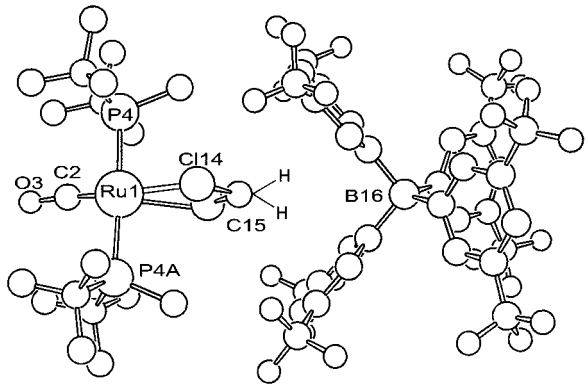

Figure 2. PLUTO plot of $[RuH(\eta^2\text{-}CH_2Cl_2)(CO)(P^tBu_2Me)_2]$-$BAr'_4$; hydrogens are omitted. Selected bond lengths (Å): Ru−Cl(14): 2.742(10), Ru−P4: 2.339(3), Ru−C2: 1.727(27), Cl(14)−C(15): 1.756(27), C2−O3: 1.228(26). Bond angles (deg): P4−Ru−P4A: 177.0(1), P4−Ru−C(2): 86.7(8), P4A−Ru−C2: 90.6(9), Cl(14)−C(15)−Cl(14A): 109.0(5), Cl(14)−Ru−Cl(14A): 62.8(8).

In stronger coordinating solvents such as THF and diethyl ether, the reaction does not occur even though $NaBAr'_4$ is soluble in these solvents. It is likely that the solvation quenches the Lewis acidity of Na^+, which can be the major driving force for the reaction. The orange complex **2** is highly air sensitive. Moreover, filtration of the reaction mixture through a Celite pad causes partial decomposition, and no pure compound can be isolated after the filtration. To isolate **2**, the reaction solution is therefore centrifuged and the solution decanted and layered with pentane in an argon-filled glovebox. Strict exclusion of air and water is necessary. Crystals of **2** were obtained after 2 days at −20 °C. The CO stretching frequency (1951 cm^{-1}) in CD_2Cl_2 is much higher than that of **1** (1923 cm^{-1}), in accord with weaker π-back-donating ability of the metal in the former. The ^1H NMR spectrum of **2** at 20 °C in CD_2Cl_2 shows two virtual triplets for diastereotopic ^{t}Bu, one virtual triplet for PCH_3 and a triplet at −19 ppm for the hydride. Also seen is a single BAr'_4 ($Ar' = 3,5\text{-}C_6H_3(CF_3)_2$) environment. The lower chemical shift of the hydride compared to that of **1** (−25 ppm) was the first indication of some weak ligand trans to the hydride; methylene chloride is one candidate. However, attempts failed to detect the coordination of CH_2Cl_2 by ^{13}C NMR spectroscopy even at − 95 °C. Therefore, an X-ray crystal structure determination is essential to define the composition and structure of the product.

A well-formed single crystal of $[RuH(CO)L_2][BAr'_4]\cdot 2CH_2Cl_2$ grown from CH_2Cl_2/pentane shows the unit cell to contain one CH_2Cl_2 molecule in the lattice, in the general region of the Ar′ rings, and the other CH_2Cl_2 donating both chlorines to Ru(II), to complete a six-coordinate octahedral geometry about the metal (Figure 2). The structural parameters support weak coordination of CH_2Cl_2. The Ru/Cl distances are long (2.74 Å), as in CH_2Cl_2 adducts of other platinum metals.[20] The C−Cl distance (1.756(27) Å) and angle (109.0(5)°) are only slightly different from those in free CH_2Cl_2 (1.772 Å and 111.8°, gas phase).[21] The Cl−Ru−Cl angle is quite acute (63°), comparable to that of the η^2-CH_2Cl_2 adduct of Ag(I).[22] It is particularly noteworthy that the BAr'_4 anion interacts in a pairwise space-filling manner with the cation: two phenyl rings adopt an atypical rotational conformation about the B−C(*ipso*) bond to form a crevice, into which the CH_2Cl_2 ligand fits like a knife-edge. This directs each (acidic) dichloromethane hydrogen toward the center of a phenyl ring, to form a hydrogen bond to the arene π-system.[23] The calculated distance of a CH_2Cl_2 hydrogen to the center of the Ar′ ring is 2.74 Å. Thus, even in the solid state, an intimate ion pair is formed, with CH_2Cl_2 acting as a bridge between cation and anion. The bridge, however, is weak. Under dynamic vacuum for 12 h, a solvent-free complex is obtained. Elemental analysis of the resulting solid is in agreement with the solvent-free form. Moreover, the ^1H NMR spectrum of this solid in CD_2Cl_2 does not show a signal for CH_2Cl_2.[24] Accordingly, a much higher CO stretching frequency (1971 cm^{-1}, Nujol) than that in CD_2Cl_2 solution also indicates even less back-donation from the metal center in the solvent-free form. Two IR bands at 2722 and 2672 cm^{-1} are found for the solvent-free product and are assigned to two agostic C−H bonds from the phosphines. The agostic interaction may provide enough stabilization to compensate the energy cost of losing coordinated CH_2Cl_2, which is not essential in the synthesis of the solvent-free complex since the same complex can also be synthesized independently in C_6H_5F (Scheme 1).

An X-ray diffraction study of this CH_2Cl_2-free material (Figure 3), **3**, shows no interaction of either the lattice C_6H_5F or the BAr'_4 anion with the cation. The $RuH(CO)L_2^+$ ion has thus been authentically "isolated", although the cation in the crystal is disordered around a center of symmetry, which limits information on the quantitative features of the structure. The phosphines bend toward one another (P−Ru−P = 166.3(5)°), and for each phosphine, one ^{t}Bu group bends inward, toward Ru (Ru−P−C = 100.3(5)° and 96.4(5)° compared to 119.7(8)° and 116.4(8)° for the second ^{t}Bu groups). As a result, there are two short Ru/$CH_3(^tBu)$ distances (2.74-(2) and 2.85(2) Å), which speak for the 14-electron $RuH(CO)L_2^+$ forming two cis agostic interactions to methyl C−H bonds. The authentic 14-electron species is thus too electron deficient to exist without agostic interaction when $L = P^tBu_2Me$. Removal of the OTf does not cause a large change of the relative positions of phosphine and CO. However, since the hydride is not located, further comparison between $RuH(CO)L_2^+$ and its triflate is not possible.

Reactivity of $[RuH(CO)L_2]BAr'_4$. This highly unsaturated complex exhibits some interesting reactivity that is not possible for its less electrophilic five-coordinated precursor $RuH(OTf)(CO)L_2$.

(A) Diethyl Ether. In the presence of ca. 1 equiv of diethyl ether at −80 °C a 1:1 diethyl ether adduct, **4a**, is observed when **2** is dissolved in methylene chloride (Scheme 1). The ^1H NMR spectrum of **4a** gives a high-

(20) (a) The Pt−Cl(CH_2Cl) distance is 2.489(4) Å: Butts, M. D.; Scott, B. L.; Kubas, G. J. *J. Am. Chem. Soc.* **1996**, *118*, 11831. (b) The Ir−Cl(CH_2Cl) is 2.462(3) Å; see: Arndtsen, B.; Bergman, R. G. *Science* **1995**, *270*, 1970.

(21) Myers, R. J.; Gwinn, W. D. *J. Chem. Phys.* **1952**, *20*, 1420.

(22) Newbound, T. D.; Colsman, M. R.; Miller, M. M.; Wulfsberg, C. P.; Anderson, O. P.; Strauss, S. H. *J. Am. Chem. Soc.* **1989**, *111*, 3762.

(23) Steiner, T.; Starikov, E. B.; Amado, A. M.; Teixeira-Dias, J. J. C. *J. Chem. Soc., Perkin Trans. 2* **1995**, 1321.

(24) CH_2Cl_2 in CD_2Cl_2 is a singlet at 5.34 ppm, different from $CDHCl_2$, which is a triplet at 5.33 ppm.

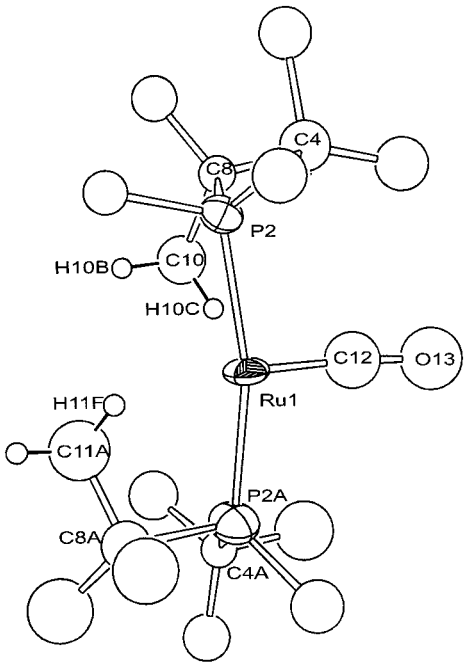

Figure 3. ORTEP diagram of $[RuH(CO)(P^tBu_2Me)_2]^+$. Hydrogens are omitted except the ones on agostic carbons. Selected bond lengths (Å): Ru1−P2: 2.403(6), Ru1−P2A: 2.332(7), Ru1−C12: 1.69(2), Ru1−C10: 2.85(2), Ru1−C11A: 2.74(2). Bond angles (deg): P2−Ru1−P2A: 166.3(5), Ru1−P2A−C8A: 96.4(8), Ru1−P2A−C4A: 116.4(8), Ru1−P2−C4: 119.7(8), Ru1−P2−C8: 100.3(5). Ru1−C12−O13: 174(2).

Scheme 2

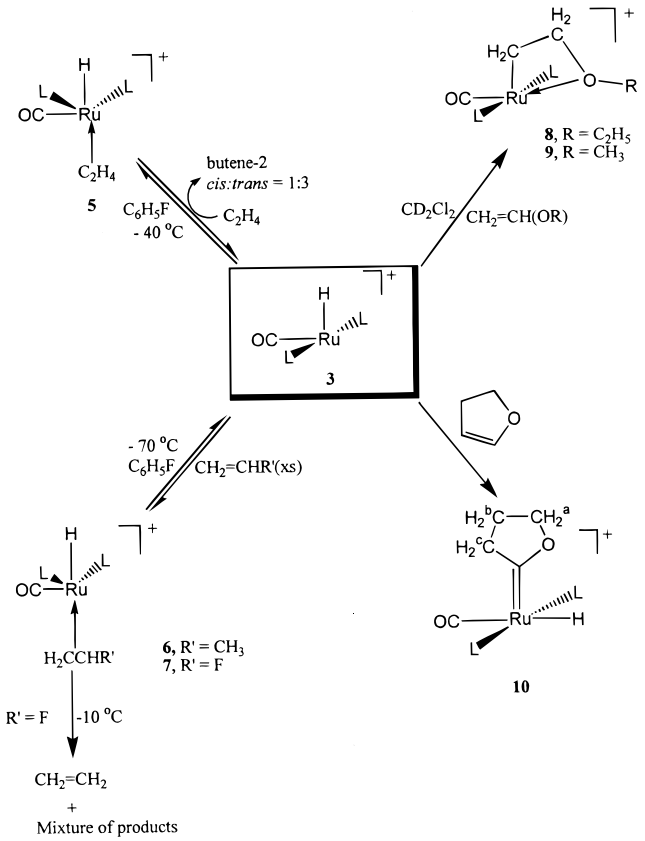

field shifted hydride triplet (−26 ppm, J_{PH} = 18 Hz) and two quartets for methylene protons at lower field (3.74, 3.58 ppm) than that of free diethyl ether (3.35 ppm). The two CH_2 peaks are attributed to slow rotation about the Ru−O bond, and the two ethyls are inequivalent, with one ethyl above and the other below the basal plane. The $^{31}P\{^1H\}$ NMR spectrum of **4a** is a singlet at 55 ppm, close to that of **1** (56 ppm). The fact that **4a** can be formed in large excess of CD_2Cl_2 (solvent) reveals that diethyl ether is a much better ligand than bidentate CD_2Cl_2. At room temperature, the coordinated diethyl ether ^1H NMR peaks coalesce with those of free diethyl ether, and the hydride signal moves to lower field (−21 ppm) as a broad peak. So does the $^{31}P\{^1H\}$ NMR peak (52 ppm). Thus the adduct is in equilibrium with the methylene chloride adduct, **2**, at room temperature.

(B) H_2O. If 1 equiv of water is added to a CD_2Cl_2 solution of **2**, an adduct, $[RuH(OH_2)(CO)L_2]BAr'_4$, **4b**, is formed cleanly (Scheme 1). Spectroscopic evidence for **4b** includes a broad singlet (^1H NMR) at 3.17 for coordinated H_2O and an upfield triplet for a hydride (−25 ppm, J_{PH} = 22.4 Hz). The O−H stretching frequency is located at 3632 and 3550 cm^{-1}, and the CO stretching frequency (1950 cm^{-1}) is also almost identical to that of **2**. The coordinated water binds stronger than does methylene chloride and cannot be removed under vacuum.

(C) Ethylene. At −40 °C under 1 atm of ethylene, in a 4:1 mixture of C_6H_5F and C_6D_{12}, an adduct $[RuH(\eta^2\text{-}CH_2CH_2)(CO)L_2]BAr'_4$, **5**, is formed quantitatively, (Scheme 2). **5** has a hydride triplet at much lower field (−3.13 ppm) than that of **4a/b**, indicating the site trans to the hydride is occupied. Compared to the free ethylene (5.40 ppm), the coordinated ethylene protons appear at higher field (3.12 ppm) with integration of four protons (vs the hydride). One singlet in the $^{31}P\{^1H\}$ NMR spectrum and two virtual triplets for ^{t}Bu protons reveal the two phosphines are mutually trans. At this temperature, a small amount of butene-1 and butene-2 is observed. When the temperature is raised to −20 °C, more ethylene is converted to butene-1 and butene-2. On further warming to 10 °C, all ethylene and butene-1 disappear and only free butene-2 and $[RuH(\eta^2\text{-}CH_2{=}CH_2)(CO)L_2]^+$ are observed. ^1H NMR analysis of the volatiles shows it to contain *cis*- and *trans*-butene-2 with a 1:3 ratio. If more ethylene (1 atm) is added to the same tube, dimerization continues. However, the catalyst decomposes at room temperature after 12 h and the dimerization ceases. The total turnover number from the NMR tube experiment is 16 (ethylene per metal). In CD_2Cl_2 at −80 °C, a 1:1 adduct is observed with different chemical shifts of the coordinated C_2H_4 (3.62 ppm) and the hydride (−2.72 ppm). Moreover, no ethylene dimer is observed in this solvent until the temperature rises above 10 °C, at which temperature butene-2 is formed and the ethylene is completely consumed. The slower dimerization rate indicates that competing coordination of CD_2Cl_2 inhibits the reaction at lower temperature.

(D) Propylene. At room temperature, there is no observable adduct between $[RuH(CO)L_2]^+$ and propylene, as the ^1H NMR spectrum of their mixture exhibits the features of free propylene and unchanged $[RuH(CO)L_2]^+$ in a C_6H_5F and C_6D_{12} mixture. At lower temperature (< −50 °C), a 1:1 adduct, $[RuH(\eta^2\text{-}CH_2{=}CH(Me))(CO)L_2]^+$, **6**, is formed cleanly, with a hydride signal at much lower field (−5.0 ppm, a broad apparent triplet) and an AB pattern $^{31}P\{^1H\}$ NMR spectrum (chiral

adduct). These spectral data are in accord with propylene being coordinated trans to the hydride and with significant bending of the P−Ru−P axis demonstrated by the relatively small PP′ coupling constant (165 vs 250 Hz for linear P−Ru−P). No coupling products of propylene are observed even with heat (80 °C, 2 h), which causes decomposition of $[RuH(CO)L_2]^+$.

(E) Vinyl Fluoride. Similar to ethylene and propylene, excess CH_2═CHF also forms, at −60 °C, a 1:1 adduct, $[RuH(\eta^2\text{-}CH_2{=}CHF)(CO)L_2]^+$, **7**, which is also a chiral complex. The two phosphines are inequivalent, and the $^{31}P\{^1H\}$ NMR spectrum shows an AB pattern with smaller PP coupling constant (140 Hz vs 165 Hz for the propylene adduct), indicating even more bending of the P−Ru−P angle. The ^{19}F NMR signal of the coordinated CH_2═CHF has moved strongly upfield (−150 ppm) compared to that of free vinyl fluoride (−115 ppm). A low-field hydride signal (−3.1 ppm vs −19 for **2**) reveals it is trans to the coordinated vinyl fluoride. Upon warming the solution to room temperature, free ethylene is formed along with at least seven phosphine-containing products (Scheme 2). Some of these are doublets by $^{31}P\{^1H\}$ NMR, with coupling constants around 20 Hz, presumably to fluorine on Ru.

(F) Vinyl Ether. Addition of 1 equiv of CH_2═CH(OEt) to $[RuH(CO)L_2]BAr'_4$ in fluorobenzene at 25 °C causes an immediate color change to darker orange. NMR spectroscopic data reveal clean formation of $[Ru(CH^a{}_2CH^b{}_2OCH^c{}_2CH^d{}_3)(CO)L_2]BAr'_4$, **8**. The ^1H NMR spectrum shows a triplet (3.81 ppm, J_{HH} = 8 Hz) for H^b and a quartet (3.14 ppm, J_{HH} = 7.2 Hz) for H^c. Correspondingly, H^a appears as a triplet of triplets (1.88 ppm, $J_{HH} = J_{PH}$ = 8 Hz) and H^d is a triplet (0.85 ppm, J_{HH} = 7.2 Hz). In the $^{13}C\{^1H\}$ NMR spectrum, the $CH_2CH_2OCH_2CH_3$ carbons are located at 85.2, 70.4, 13.2 ($CH^d{}_3$), and −0.67($CH^a{}_2$) ppm, respectively. However, these data are not decisive about ether oxygen coordination to Ru. Attempts to grow a single crystal for X-ray diffraction study failed, as the complex is decomposed slowly in fluorobenzene/pentane solution even at −40 °C. Methyl vinyl ether reacts similarly to form an inserted product, $[Ru(CH_2CH_2OMe)(CO)L_2]^+$, **9**, which was crystallized from a fluorobenzene/pentane mixture. Spectroscopically, it has features similar to those of **8**. Crystal structure determination shows that the oxygen is coordinated (Figure 4) with a Ru−O(ether) distance of 2.226(8) Å, longer than that of **1** (2.2088(9) Å). If **9** is dissolved in diethyl ether, the reverse reaction occurs to give **4a** and free CH_2═CH(OMe), which indicates no strong thermodynamic preference for the substituted ethyl complex.

(G) Reaction Mechanism of $[RuH(CO)L_2]^+$ with CH_2═CH(OEt). To detect any intermediates, this reaction was monitored by low-temperature NMR spectra in CD_2Cl_2. Figure 5 depicts the variable-temperature $^{31}P\{^1H\}$ NMR spectra of the 1:1 mixture of **3** and CH_2═CH(OEt). After 30 min of mixing at −80 °C, one major product, **11**, is formed (Scheme 3), which has an AB pattern $^{31}P\{^1H\}$ spectrum (J_{PP} = 224 Hz). This P/P coupling is characteristic of little bending of ∠P−Ru−P, and thus of vinyl ether binding cis to hydride, and as a σ donor. In the ^1H NMR spectrum at the same temperature, one hydride is detected at very high field (−28.0 ppm) as an apparent triplet (J_{PP} = 14 Hz). This

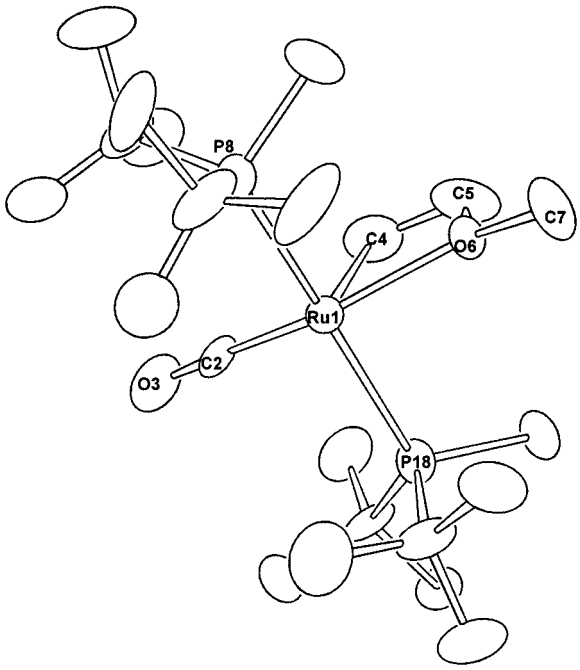

Figure 4. ORTEP diagram of $[Ru(\eta^2\text{-}CH_2CH_2OMe)(CO)(P^tBu_2Me)_2]^+$ All hydrogens are omitted for clarity. Selected bond distance (Å): Ru1−C2: 1.796(15), Ru1−C4: 2.068(13), Ru1−O6: 2.226(8), Ru1−P8: 2.409(7), Ru1−P18: 2.411(7). Bond angles (deg): C2−Ru1−C4; 94.0(7), C2−Ru1−O6: 157.0(13), C4−Ru1−O(6): 63.2(14), C2−Ru1−P(8): 91.4(4), P8−Ru1−P18: 172.5(3), C5−C4−Ru1; 96.2(9).

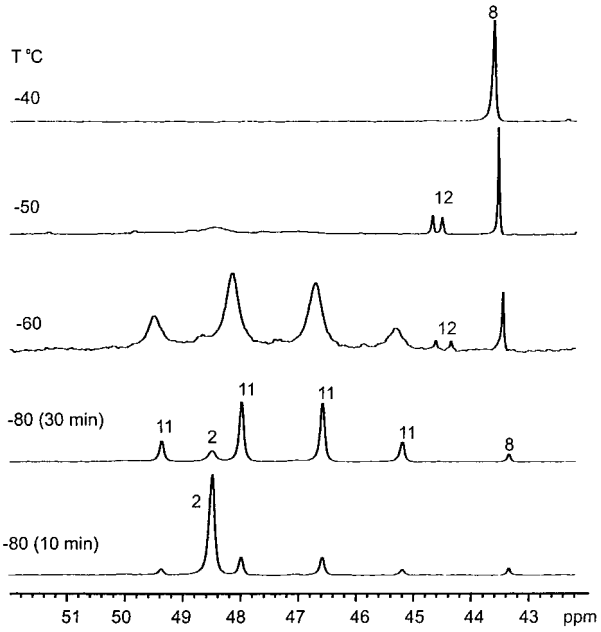

Figure 5. Variable-temperature $^{31}P\{^1H\}$ NMR spectra of $[RuH(CD_2Cl_2)(CO)L_2]BAr'_4$, **2**, plus $CH_2CH(OEt)$. Solvent: CD_2Cl_2. Peaks are labeled with complex numbers.

indicates the hydride is trans to a vacant site. The α-H of the vinyl ether is shifted to lower field (7.3 ppm) in comparison to that (6.5 ppm) of free CH_2═CH(OEt). The β-protons also shifted slightly downfield from that of free vinyl ether. These spectral data are consistent with O→Ru binding, not a π-adduct through the C═C bond; the latter would have resulted in high-field shifts of the vinylic protons. The AB pattern $^{31}P\{^1H\}$ NMR is likely due to hindered rotation around the Ru−P axis caused

Scheme 3

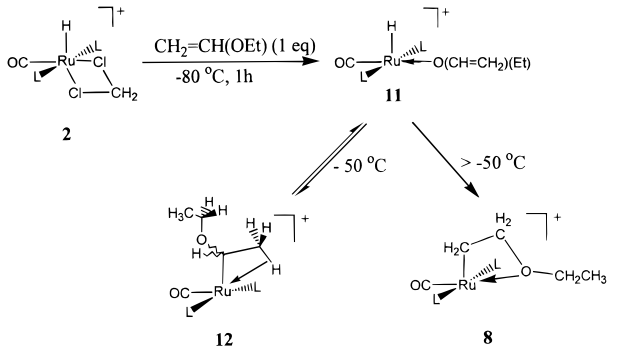

by steric hindrance in the adduct. Hindered rotation is a fairly common phenomenon in five- or six-coordinated $Ru(P^tBu_2Me)_2$ complexes, especially at low temperature.[25] Upon warming to −60 °C, the AB lines broaden, together with formation of two new compounds, **8** and **12**. Further warming to −50 °C for 30 min (Figure 5) resulted in conversion of the adduct to **8** and **12** (AB pattern, $J_{PP} = 202$ Hz) (Scheme 3). The latter is chiral, and thus the two phosphines are chemically inequivalent. The structure assigned to **12** is further supported by the ^{1}H NMR spectrum at the same temperature. A broad peak is observed at 5.5 ppm for the α-H, and the most characteristic peaks are the diastereotopic methylene protons of OCH_2Me, which appear at 3.55 and 3.37 ppm as two apparent quintets ($J_{HH} = 8.4$ Hz). A singlet peak at relatively high field (0.4 ppm) is observed for β CH_3 protons. The high-field shift is very likely due to β-agostic interactions. **12** is a short-lived species; as the temperature warmed further to −40 °C, it disappears and **8** is the only observed product.

(H) 2,3-Dihydrofuran. In sharp contrast to the reaction of acyclic vinyl ethers, the cyclic vinyl ether 2,3-dihydrofuran reacts with $[RuH(CO)L_2]^+$ in C_6H_5F to give a carbene complex, **10**, in over 90% yield in 1 h at 20 °C (Scheme 2). The most characteristic feature for the carbene complex is a low-field peak (302.1 ppm, t, $J_{PC} = 10$ Hz) in proton-coupled ^{13}C NMR spectrum. A doublet of triplets is also located at 201.5 ppm ($^2J_{CH} = 35$ Hz and $J_{PC} = 7$ Hz); the large $^2J_{CH}$ value reveals that the hydride is trans to CO, not to the carbene. Consistently, the ^{1}H NMR spectrum of **10** has a low-field hydride peak at −1.7 ppm ($J_{PH} = 18$ Hz). Moreover, two triplets are observed at 4.2 and 2.9 ppm for CH^a_2 and CH^c_2 along with an apparent quintet at 1.5 ppm for H^b_2 (Scheme 2).

Discussion

Synthesis of $[RuH(CO)L_2]BAr'_4$. Salt metathesis of $RuH(OTf)(CO)L_2$ with $NaBAr'_4$ occurs smoothly in the time of mixing in weakly coordinating but polar solvents such as CH_2Cl_2 and fluorobenzene to give $[RuH(\eta^2\text{-}CH_2Cl_2)(CO)L_2]BAr'_4$, **2**, and $[RuH(CO)L_2]BAr'_4$, **3**, respectively. $NaBAr'_4$ has been increasingly used to generate unsaturated cationic metal complexes or their adducts with weakly coordinated solvents.[26,20a] The reaction here does not go in polar but more coordinating solvents such as THF and diethyl ether, despite the high solubility of $NaBAr'_4$ in these solvents. It is likely that the solvent coordinates the sodium cation and decreases its Lewis acidity. The insolubility of NaOTf in methylene chloride or fluorobenzene is another factor promoting reaction. Qualitatively, the reaction is also highly dependent on the particle size of $NaBAr'_4$. Very fine powders are much more effective than larger ones. If the reaction is not complete, the ^{1}H and ^{31}P NMR spectra give deceptively simple spectra at room temperature: the spectra show coalesced peaks of the signals from **1** and **2** (or **3**). Depending on the molar ratio of **1** and **2** (or **3**) in the mixture, the ^{31}P NMR spectrum peak falls between 56 and 49 (in CD_2Cl_2) or 56−46 (C_6H_5F). Low-temperature ^{1}H or ^{31}P NMR spectra do however give decoalesced signals of **1** and **2** (or **3**). **2** and **3** can be isolated as orange crystals by layering the reaction solution with pentane at −20 °C. Upon separation from the solvent, **2** readily loses CH_2Cl_2 under vacuum to give **3**, which decomposes slowly under argon at room temperature. Both compounds are extremely air sensitive, and in order to isolate pure compound, all the reaction solvents must be strictly dried and degassed before use and the manipulations are best carried out in an argon-filled glovebox to avoid contact with air.

Structure of $[RuH(CO)L_2]^+$. The X-ray crystal structure of the cation shows that it has two trans phosphine ligands. Two agostic interactions (discussed previously)[10] are also obvious from the two abnormally small Ru−P−C(tertiary) angles (96.4° and 100.3° vs 116.4° and 119.7° for those not involved in agostic interactions), the agostic interactions are cis to each other, and so the undetermined hydride must be cis to CO. DFT calculations have been carried out to provide a geometry of the complex and in particular locating H.[10] It has been found that the angle H−Ru−CO is 87° in the absence of CH_2Cl_2 and 85° in the presence of coordinated CH_2Cl_2. It can thus be assumed that the structure of $RuH(CO)(P^tBu_2Me)_2^+$, in which two agostic bonds are present, also has the same overall skeleton.

Reactions of 3 with Ethylene. Although there are two vacant sites of **3**, it forms only a 1:1 adduct not only with diethyl ether but also with ethylene. While the diethyl ether or H_2O adduct has the hydride trans to the vacant site, the observed ethylene adduct has coordinated C_2H_4 trans to the hydride, evidenced by much lower field hydride chemical shift (−3.1 vs −23 ppm of **3**). Coordination site preferences have been studied by DFT calculations (see the following paper), and there is very little site preference to $RuH(CO)L_2^+$, at least for L = PH_3.

Ethylene is catalytically dimerized in fluorobenzene to give butene-1 and butene-2 at low temperature (−40 °C). Thus two C_2 fragments must sometimes be simultaneously on Ru. No higher molecular weight oligomers are detected. Apparently, this Ru(II) does not allow the polymer chain to grow. In CD_2Cl_2 the ethylene dimerization reaction does not occur until much higher temperature (>10 °C). The solvent dependency is most likely due to competion of CD_2Cl_2 with ethylene for binding to Ru. On the basis of the experimental observation, we propose the formation mechanism of butene as follows (Scheme 4): First, coordinated ethylene (cis to hydride) inserts into Ru−H bond to give ethyl

(25) Notheis, J. U.; Heyn, R. H.; Caulton, K. G. *Inorg. Chim. Acta* **1995**, *229*, 187.
(26) Heinekey, D. M., Radzewich, C. E. *Organometallics* **1998**, *17*, 51.

Scheme 4[a]

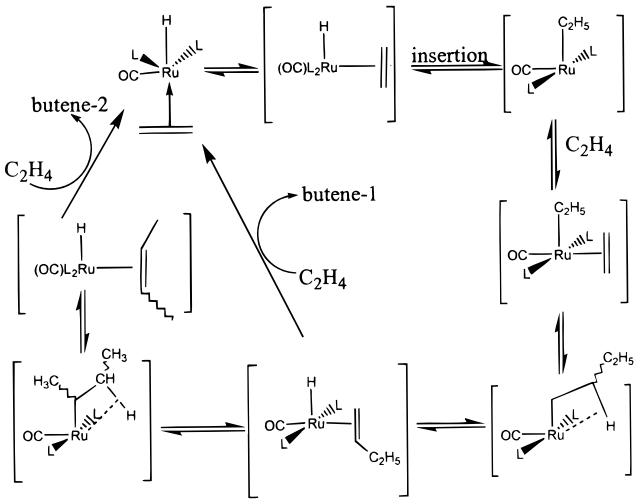

[a] All complexes have +1 charge.

complex. Then a second ethylene inserts to give a β-agostic butyl complex. β-H elimination leads to a butene-1 complex of **3**. Butene-1 can be replaced by C_2H_4 or isomerized to butene-2 by insertion and β-H elimination. An independent experiment shows that **3** catalyzes isomerization of butene-1 to butene-2 (1:3 cis and trans mixture) under the same conditions as that of dimerization of C_2H_4. The selectivity of the final isomerization product is governed by the relative stability of the *free* internal alkene vs the terminal alkene.

Reaction with Acyclic and Cyclic Vinyl Ethers: Contrasting Thermodynamic Products. Low-temperature NMR spectra (−80 °C) of $[RuH(CO)L_2]^+$ with equimolar ethyl vinyl ether in CD_2Cl_2 indicates that the ether coordinates trans to CO through oxygen (**11**) (Scheme 3) instead of the C=C bond as in the ethylene adduct. The metal preference for non π-acidic ligand (oxygen) further reveals that $[RuH(CO)L_2]^+$ is a strong electrophile and a weak π-base. Insertion occurs at higher temperature (−60 °C) to give two alkyl products in comparable rate. One has the OEt group at the α-carbon and a β-H agostic bond (**12**) and the other has OEt at the β-carbon with oxygen coordinated to Ru, **8**, as revealed by the X-ray structure determination. **12** is converted to **8** on further warming to −40 °C (Scheme 3). The thermodynamics of this reaction are not so obvious because from **11** to **8** the Ru electron count remains that same. However, **8** has a four-membered ring; thus the oxygen may not be coordinated as well as that in **11**. Precisely this inability to predict relative energies motivated the computational study in the following paper. Changing the vinyl ether to a cyclic one could discourage the oxygen chelation due to the ring constraint. Indeed, 1,2-dihydrofuran reacts with $[RuH(CO)L_2]^+$ to give carbene **10**. The alkyl product, **13**, is not observed.

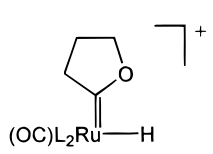

10

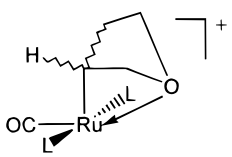

13

Scheme 5

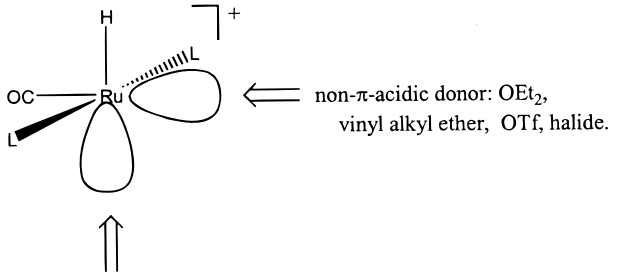

$[RuHClL_2]$ vs $[RuH(CO)L_2]^+$. It has been demonstrated that 14-electron $RuHCl(P^iPr_3)_2$ coordinates one ethyl vinyl ether to give $RuHCl(\eta^2\text{-}CH_2{=}CH(OEt))(P^iPr_3)_2$ below −65 °C, and the vinyl ether coordinates trans to chloride through the C=C bond.[1,2] At higher temperature (> 0 °C) the adduct isomerizes to carbene, $RuHCl(=C(OEt)Me)(P^iPr_3)_2$. In this case, the metal π-basicity controls the thermodynamics of the reaction.[1]

Conclusion

Formally 14-electron $[RuH(CO)(P^tBu_2Me)_2]BAr'_4$ is synthesized by salt metathesis of $RuH(OTf)(CO)L_2$ and $NaBAr'_4$ in the noncoordinating but polar solvent fluorobenzene. The cation has sawhorse geometry, with two vacant sites occupied by the C−H bond of phosphine ligands. The preferred geometry is determined by the electronic configuration of Ru, which prefers to stay at a low-spin state, particularly in the presence of the strong-field ligands hydride and CO. The cationic charge and the strong π-acid CO significantly weaken the metal π-basic character but strengthen its σ-acidity. The reactivity of this complex also testifies to this conclusion. $[RuH(CO)L_2]^+$ only binds CH_2Cl_2 in η^2 fashion but does not oxidatively add to the C−Cl bond. It does not merely form a stable adduct with π-acidic ethylene but also dimerizes it. Selective coordination with vinyl ether oxygen and the thermodynamics of the subsequent insertion and isomerization reactions further manifest the strong Lewis acidity and weakened π-basicity of the Ru cation. The different coordination geometry of $[RuH(CO)L_2]^+$ with π-acids and non-π-acidic ligands reveals that the two low-lying empty orbitals are significantly different: the site trans to CO prefers a pure donor ligand, and the site trans to H prefers a π-acidic ligand (Scheme 5). In this context, it is interesting that vinyl ethers initially bind through oxygen (and trans to CO) rather than through the C=C bond. The magnitude of the site preference is evaluated in the accompanying paper.

The results reported here show that, while $RuH(CO)(P^tBu_2Me)_2^+$ has a π-basicity less than that of $RuHCl(P^iPr_3)_2$, as evidenced by its ability to coordinate Lewis base ligands, it still has the ability to transform selected vinyl ethers to carbene complexes. However, unlike $RuHCl(P^iPr_3)_2$ it also has the ability to isomerize other vinyl ethers to hydrogenated (β-alkoxyethyl) ligands. Finally, the regioselectivity for adding Ru−H across the C=C bond of a vinyl ether is demonstrated to be under thermodynamic control, since the primary product at −50 °C is observed to isomerize to the η^2-β-methoxyethyl isomer upon warming. This richly varied behavior

Table 1. Crystallographic Data

	1	2	3	9
formula	$C_{20}H_{43}F_3O_4P_2RuS$	$C_{53}H_{58}BCl_4F_{24}OP_2Ru$	$C_{57}H_{60}BF_{25}OP_2Ru$	$C_{57}H_{62}BF_{24}O_2P_2Ru$
a, Å	8.085(2)	13.639(1)	18.744(3)	13.622(1)
b, Å	15.004(3)	13.639(1)	17.870(3)	13.622(1)
c, Å	22.718(5)	34.558(3)	18.608(3)	34.616(3)
α, deg	90.00(0)	90.00(0)	90.00(0)	90.00(0)
β, deg	90.81(1)	90.00(0)	95.48(1)	90.00(0)
χ, deg	90.00(0)	90.00(0)	90.00(0)	90.00(0)
V, Å^3	2755.58	6429.24	6204.09	6423(2)
Z	4	4	4	4
fw	599.64	1482.64	1408.88	1408.9
space group	$P2_1/c$	$P4_12_12$	$C2/c$	$P4_12_12$
temp, °C	−169	−170	−170	−174
λ, Å	0.71069	0.71069	0.71069	0.71069
ρ_{calcd} g/cm^3	1.445	1.532	1.508	1.455
μ(Mo Kα), cm^{-1}	8.034	5.580	4.075	3.918
R^a	0.03	0.046	0.079	0.0663
R_w	0.032	0.044	0.130[c]	0.1574[c]

[a] $R = \sum||F_o| - |F_c||/\sum|F_o|$. [b] $R_w = [\sum w(|F_o| - |F_c|)^2/\sum w|F_o|^2]^{1/2}$ where $w = 1/\sigma^2(|F_o|)$. [c] On F^2.

toward olefins will be interpreted by DFT calculations as due to a subtle interplay of ligands at the metal and the substituent on the olefin.

Experimental Section

General Procedures. All reactions and manipulations were conducted using standard Schlenk and glovebox techniques. Solvents were dried and distilled under argon and stored in airtight solvent bulbs with Teflon closures. All NMR solvents were dried, vacuum-transferred, and stored in an argon-filled glovebox. ^{1}H, ^{31}P, and ^{13}C NMR were recorded on a Varian Gem XL300 or Unity I400 spectrometer. Chemical shifts are referenced to solvent peaks (^{1}H, ^{13}C) and external H_3PO_4 (^{31}P). Infrared spectra were recorded on a Nicolet 510P FT-IR spectrometer. Elemental analyses were conducted on the Perkin-Elmer 2400 CHNS/O analyzer at the Department of Chemistry, Indiana University. RuHCl(CO)L_2[27] and RuHF(CO)L_2[15] were synthesized by a literature method. NaBAr′$_4$ is prepared following Brookhart and co-workers' procedure.[28] Other chemicals are commercially available and used as received or degassed before use. Compounds for which combustion analyses are not shown are either thermolabile, transient intermediates, or closely related to analogous species.[1,2,10]

RuH(OTf)(CO)(P^{t}Bu$_2$Me)$_2$, 1. RuHF(CO)L_2 (2.0 g, 4.3 mmol) was dissolved in dry diethyl ether (30 mL). To the solution, Me_3SiOTf (0.83 mL, 43 mmol) was slowly added via a syringe. An exothermic reaction occurred immediately. In the case of fast addition, reflux of the solvent is observed. The solution color changed to bright yellow. After the addition (5 min), the solution was stirred for 10 min and the volatiles were removed in vacuo. The residue was recrystallized from diethyl ether (−40 °C) to yield yellow needles, 2.2 g (92%). Anal. Calcd for $C_{20}H_{43}F_3O_4P_2RuS$: C, 40.06; H, 7.23. Found: C, 40.40; H, 6.95. ^{1}H NMR (C_6D_6, 20 °C): 1.48 (vt, N = 5.1 Hz, PCH_3), 1.13 (vt, N = 13 Hz, 18H, $PC(CH_3)_3$), 1.00 (vt, N = 13 Hz, 18H, $PC(CH_3)_3$), −24.7 (t, J_{PH} = 19 Hz, 1H, Ru−H). ^{31}P{^{1}H} NMR (C_6D_6, 25 °C): 56.4 (s). ^{19}F NMR (C_6D_6, 25 °C): −76.6 (CF_3SO_3). IR (C_6D_6, cm^{-1}): ν(CO) = 1923.

Crystal Structure Determination of 1. Crystals were grown from diethyl ether at −20 °C. A suitable crystal was mounted in a nitrogen atmosphere glovebag using silicone grease. The crystal was then transferred to the goniostat, where it was cooled to −169 °C for characterization and data collection. An automated search of selected regions of reciprocal space followed by analysis using the programs DIRAX and TRACER gave a monoclinic primitive unit cell. After complete intensity data collection the systematic extinction of 0*k*0 for $k = 2n + 1$ and of *h*0*l* for $l = 2n + 1$ uniquely identified the space group as $P2_1/c$. The structure was solved using a combination of direct methods (MULTAN-78) and Fourier techniques. The Ru atom position was obtained from the initial E-map. The remaining non-hydrogen atoms were located in iterations of least-squares refinement and difference Fourier calculations. Almost all of the hydrogen atoms were located, they were initially included in fixed idealized positions, and later refined with isotropic thermal parameters. Near the conclusion of the refinement a possible hydride atom H(43) was introduced. The peak had appeared consistently in several difference maps. The final $R(F)$ = 0.031 for the 410 total variables and using all of the unique data. The largest peak in the difference map was 0.59 e/Å^3 near Ru(1), and the deepest hole was −0.79 e/Å^3. The crystallographic parameters are listed in Table 1.

[RuH(η^2-CH$_2$Cl$_2$)(CO)(P^{t}Bu$_2$Me)$_2$][BAr′$_4$], 2. RuH(OTf)(CO)(P^{t}Bu$_2$Me)$_2$ (200 mg, 0.33 mmol) was mixed with NaBAr′$_4$ (300 mg, 0.34 mmol) in an test tube (10 mL, with a Teflon-lined screw cap). To the mixture was added CH_2Cl_2 (5 mL). After shaking for 5 min, the orange solution was centrifuged and decanted to a Schlenk tube and layered with pentane. The solution was kept at −20 °C for one week to form large orange crystals. The crystals were filtered, washed with pentane, and dried briefly. ^{1}H NMR (CD_2Cl_2, 20 °C): 7.7(s, 8H, BAr′$_4^-$), 7.50 (br s, 4H, BAr′$_4^-$), 5.34 (s, CH_2Cl_2), 1.54 (vt, N = 4.8 Hz, 6H, PCH_3), 1.30 (vt, N = 14.4 Hz, 18H, P^{t}Bu), 1.13(vt, N = 13.2 Hz, 18H, P^{t}Bu), −19.4 (br t, J_{PH} = 17 Hz, 1H, Ru−H). ^{31}P{^{1}H} NMR (CD_2Cl_2, 20 °C): 49 (s). ^{19}F NMR (CD_2Cl_2, 20 °C): −62.0 (s). IR (CD_2Cl_2, cm^{-1}): ν(CO) = 1951.

X-ray Crystal Structure Determination of [RuH(η^2-CH$_2$Cl$_2$)(CO)(P^{t}Bu$_2$Me)$_2$]BAr′$_4$, 2. The X-ray quality crystals were grown from methylene chloride and pentane at −20 °C. The crystals were highly air-sensitive, readily lost solvent, and decomposed upon warming to room temperature. A large clump of crystals was pipetted under nitrogen to a watch glass cooled with dry ice. A small, nearly equidimensional fragment was cleaved from a larger crystal while still under the solvent and affixed to the end of a glass fiber using silicone grease. The sample was then rapidly transferred to the goniostat, where it was cooled to −170 °C for characterization and data collection. A systematic search of a limited hemisphere of reciprocal space located a set of diffraction maxima with systematic absences and symmetry corresponding to a tetragonal space group. Subsequent solution and refinement confirmed $P4_12_12$ to be the proper choice. The data were collected using a standard moving-crystal−moving-detector

(27) Gill, D. F.; Shaw, B. L. *Inorg. Chim. Acta* **1979**, *32*, 19. Huang, D.; Folting, K.; Caulton, K. G. *Inorg. Chem.* **1996**, *35*, 7035.
(28) Brookhart, M.; Grant, B.; Volpe, J. *Organometallics* **1992**, *11*, 3920.

technique with fixed backgrounds at each extreme of the scan. Data were corrected for Lorentz and polarization effects, and equivalent reflections were averaged. The structure was readily solved by direct methods (SHEXTL-PC) and Fourier techniques. All non-hydrogen atoms were refined anisotropically in the full-matrix least-squares. It was immediately obvious that the CO ligand was disordered. When the occupancies of the C and O atoms were allowed to vary, they converged rapidly to 50%, indicating one CO in two alternate cis positions. A final difference Fourier was featureless, the largest peaks, located at the F sites, being 0.8 e/A^3. The crystallographic data are listed in Table 1.

[RuH(CO)(P^{t}Bu$_2$Me)$_2$]BAr′$_4$, 3. Crystals of **2** were pumped in vacuo for 12 h to give solvent-free powder, **3**. Alternatively, this complex is obtained following the same procedure as in the synthesis of [RuH(η^2-CH$_2$Cl$_2$)(CO)(P^{t}Bu$_2$Me)$_2$]BAr′$_4$ using C_6H_5F as solvent. Yield: 40%. Anal. Calcd for $C_{51}H_{55}BF_{24}OP_2Ru$: C, 46.57; H, 4.22. Found: C, 46.15, H, 4.33. IR (Nujol, cm^{-1}): 2722, 2672 (agostic ν(C−H)), 1971 (ν(CO)). ^{1}H NMR (C_6D_5F, 300 MHz, 20 °C): 8.24 (br s, 8H, Ar′), 7.62 (br s, 4H, Ar′), 1.09 (vt, N = 5.2 Hz, 6H, PCH$_3$), 0.91 (vt, N = 14 Hz, 18H, P^{t}Bu), 0.88 (vt, N = 13 Hz, 18H, P^{t}Bu), −23.0 (t, J_{PH} = 20 Hz, Ru−H). ^{31}P{^{1}H} NMR (121 MHz, 20 °C): 46.6 (s).

Structure Determination of [RuH(CO)(P^{t}Bu$_2$Me)$_2$]-BAr′$_4$, 3. X-ray quality crystals were grown from fluorobenzene and pentane at −20 °C. A small, single crystal was selected from the bulk sample and affixed to the tip of a glass fiber with the use of silicone grease. The mounted sample was then transferred to the goniostat and cooled to −165 °C for characterization and data collection. The sample was handled under nitrogen atmosphere at dry ice temperature to prevent decomposition and solvent loss. A systematic search of a limited hemisphere of reciprocal space located a set of data with monoclinic symmetry and systematic absences that correspond to the centrosymmetric space group *C*2/*c* or the noncentrosymmetric space group *Cc*. Subsequent solution and successful refinement of the structure suggest the centrosymmetric choice. Data were collected by the moving-crystal−moving-detector technique with fixed background counts at each extreme of the scan. Data were corrected for Lorentz and polarization effects. The structure was solved by direct methods (SHELXTL) and Fourier techniques. Hydrogen atoms were placed in calculated positions and refined with the use of a riding model. All non-hydrogen atoms were refined anisotropically except for the carbon atoms of the disordered phosphine ligands. The distinction between centric/acentric space groups deserves some comment. In the final model in *C*2/*c*, the entire cation is disordered about a center of symmetry, with the Ru atom only about 0.3 Å away from it. This could be interpreted as an indication that the chosen space group symmetry is too high. However, refinement in the acentric space group produces a model in which the anion and solvent molecules contain near precise, but noncrystallographic (in *Cc*), 2-fold axes; the anisotropic thermal parameters behave poorly, and correlation is problematic. In the centric model, the anion and C_6H_5F solvent molecules each contain a crystallographic 2-fold axis; anisotropic thermal parameters refine well, except for the carbon atoms in the disordered phosphine ligands, and there are no significant correlation problems. Difficulty with anisotropic thermal parameters in the disordered cation can be attributed to near-overlap of the two components of the disorder. Even in the seemingly ordered *Cc* model, a large disparity in the Ru−P bond lengths suggests a disorder of the ruthenium. Also, the phosphine carbon atoms in the *Cc* model were much more difficult to locate and refine than were the other carbon atoms in the structure. The cation disorder thus seems to carry over into the acentric model, and there is no advantage to selecting *Cc* as the space group. While the presence of a hydride can neither be confirmed nor denied based on the X-ray results, there is an open space in the ruthenium atom coordination sphere, cis to the CO, for the hydride. A final difference Fourier map was featureless, with the largest peak having an intensity of 0.49 e/Å^3 and residing near the ruthenium atom. The crystallographic data are collected in Table 1.

[RuH(OEt$_2$)(CO)(P^{t}Bu$_2$Me)$_2$]BAr′$_4$. [RuH(CO)L$_2$]BAr′$_4$ (20 mg, 1.4 × 10^{-2} mmol) was dissolved in CD_2Cl_2 (0.5 mL). To the solution was added diethyl ether (1.4 μL). ^{1}H NMR (400 MHz, −80 °C): −26.0 (t, J_{PH} = 18 Hz, Ru−H), 1.18 (br, P^{t}Bu), 1.25 (br, P^{t}Bu), 3.58 (q, J_{HH} = 5.2 Hz, 2H, OCH$_2$), 3.75(q, J = 5.6 Hz, 2H, OCH$_2$), 7.55 (s, 4H, *para*-H of Ar′), 7.77 (s, 8H, *ortho*-H of Ar′). ^{31}P{^{1}H} NMR (162 MHz, −80 °C): 55.0 (s). Upon warming to 20 °C, the phosphine peak shifted to 51.2 ppm, and the hydride peak moves to −21.3 ppm as a broad line. The methylene proton peaks for coordinated OEt$_2$ coalesce with those of free (excess) OEt$_2$ to one quartet at 3.48 ppm.

[RuH(OH$_2$)(CO)(P^{t}Bu$_2$Me)$_2$]BAr′$_4$. This orange complex was first synthesized when the NaBAr′$_4$ is not sufficiently dried,[29] and then by conscious addition of stoichiometric water. The crystallization procedure is the same as that of [RuH(CO)-(PtBu$_2$Me)$_2$]BAr′$_4$. ^{1}H NMR (400 MHz, CD_2Cl_2, 20 °C): δ 7.72 (s, 8H, *ortho* H of Ar′), 7.55 (s, 4H, *para* H of Ar′), 3.17 (s, 2H, OH$_2$), 1.35 (vt, N = 6.8 Hz, 6H, PCH$_3$), 1.28 (vt, N = 14.4 Hz, 18 H, ^{t}Bu), 1.25 (vt, N = 15 Hz, 18 H, ^{t}Bu), −25.1 (t, J = 22.4, Ru−H). ^{31}P{^{1}H} NMR (162 MHz, 20 °C): δ 51.3 (s). IR (CD_2Cl_2, cm^{-1}): 3632 (ν(OH)), 3550 (ν(OH)), 1950 (ν(CO)).

Isomerization of Butene-1 by [RuH(CO)L$_2$]BAr′$_4$. [RuH-(CO)L$_2$]BAr′$_4$ (10 mg, 7.6 × 10^{-3} mmol) was dissolved in C_6H_5F (0.5 mL). The solution was degassed before butene-1 (1 atm) was added. After mixing for 5 min at room temperature, ^{1}H NMR analysis of the mixture shows no butene-1 but butene-2, with a cis:trans ratio of 1:3. ^{1}H NMR of butene-2: 1.57 (d, J = 5.4 Hz, CH$_3$ *cis*-butene-2), 1.586 (m, CH$_3$ of *trans*-butene-2), 5.41 (m, 1H, CH=CH of *trans*-butene-2), 5.48 (m, CH=CH of *cis*-butene-2).

Reaction of [RuH(CO)L$_2$]BAr′$_4$ with Ethylene in C_6H_5F. In an NMR tube [RuH(CO)(P^{t}Bu$_2$Me)$_2$]BAr′$_4$ (10 mg, 7.6 × 10^{-3} mmol) was dissolved in a 4:1 mixture of C_6H_5F and C_6D_{12} (for lock purposes). The orange solution was degassed and the tube charged with C_2H_4 (1 atm) and mixed under low temperature. The tube was transferred to a precooled NMR probe for measurements. At −40 °C, [RuH(η^2-C_2H_4)(CO)(P^{t}Bu$_2$Me)$_2$]$^+$ is formed cleanly along with a small amount of butene-1 and butene-2 (cis:trans = 1:3). ^{1}H NMR of butene-1: 5.90 (m, 1H, CH=), 5.03 (dm, J_{HH} = 17.7 Hz, ^{1}H, CH$_2$=), 4.96 (dm, J_{HH} = 9.9 Hz, ^{1}H, CH$_2$=), 2.01 (apparent quintet, J_{HH} = 6.9 Hz, CH$_2$-Me), 0.96 (t, J = 6.9 Hz, CH$_3$). NMR evidence for [RuH(η^2-C_2H_4)(CO)(P^{t}Bu$_2$Me)$_2$]$^+$: ^{31}P{^{1}H} NMR (121 MHz): 48.9 (s). ^{1}H NMR (300 MHz): 5.4 (s, free C_2H_4), 3.12 (br s, 4H, C_2H_4 coordinated), 1.18 (vt, N = 4.7 Hz, 6H, PCH$_3$), 0.924 (vt, N = 13.8 Hz, 18H, PC(CH$_3$)$_3$), 0.798 (vt, N = 14 Hz, 18H, PC(CH$_3$)$_3$), −3.13 (vt, J = 22 Hz, 1H, Ru−H). Upon warming to −20 °C, the coordinated and free C_2H_4 peak broadens and more butene-1 and butene-2 are formed. Further warming to 10 °C converts all free C_2H_4 and butene-1 to butene-2, while the ethylene adduct remains. The final molar ratio of converted C_2H_4 and metal complex is 8:1. If the tube is refilled with C_2H_4 (1 atm) and stirred at room temperature overnight, more butene-2 is formed. The turnover number (number of consumed C_2H_4 per metal complex) increases to ca. 16. However, the catalyst decomposes after 12 h at 20 °C.

Reaction of [RuH(CO)(P^{t}Bu$_2$Me)$_2$]$^+$ with Ethylene in CD_2Cl_2. The same procedure as above was followed in CD_2Cl_2 to afford [RuH(η^2-C_2H_4)(CD_2Cl_2)(CO)(P^{t}Bu$_2$Me)$_2$]BAr′$_4$. ^{1}H NMR (−50 °C, 300 MHz): 5.40 (s, free C_2H_4), 3.62 (br, 4H, coordinated C_2H_4), 1.77 (vt, N = 6.3 Hz, 6H, PCH$_3$), 1.36 (vt, N = 15 Hz, 18H, PC(CH$_3$)$_3$), 0.79 (vt, N = 13.5 Hz, 18H, PC-(CH$_3$)$_3$), −2.72 (t, J_{PH} = 20 Hz, Ru−H). No butene-2 is observed at this temperature. Upon warming up to 20 °C, coordinated

(29) NaBAr′$_4$ hydrate is heated at 150 °C under vacuum for 1 day to obtain absolutely dry NaBAr′$_4$.

and free C_2H_4 are coalesced to one broad peak at 5.1 ppm and butene-2 is detected.

Reaction of [RuH(CO)L_2]$^+$ with Propylene. The same procedure was followed as in the reaction with C_2H_4 in fluorobenzene/C_6D_{12}. $^{31}P\{^1H\}$ NMR (−40 °C): 54 (d, J_{PP} = 165 Hz), 45 (d, J_{PP} = 165 Hz). ^1H NMR (−50 °C): −5.0 ppm (vt, J_{PH} = 20 Hz, Ru−H).

Reaction of [RuH(CO)L_2]$^+$ with Vinyl Fluoride. The procedure was that of the reaction with C_2H_4. ^1H NMR (300 MHz, −60 °C): −3.1 (dd, J_{PH} = 16 Hz, J_{PH} = 23 Hz, Ru−H). $^{31}P\{^1H\}$ NMR (121 MHz, −60 °C): 53.2 (d, J_{PP} = 140 Hz), 49.8 (d, J_{PP} = 140 Hz). The AB pattern peaks coalesce to a singlet at 52.1 ppm upon warming (−30 °C). As the temperature rises to −10 °C, the peak disappears and five ^{31}P signals appear. ^{19}F NMR (282 MHz, −60 °C): −150.8 (br s); this peak also broadens and disappears as the temperature rises.

[Ru(η^2-$CH_2CH_2OCH_3$)(CO)(P^tBu_2Me)$_2$]BAr′$_4$. To [RuH(CO)L_2]BAr′$_4$ (200 mg, 152 mmol) dissolved in C_6H_5F (5 mL) was added excess methyl vinyl ether, and the mixture was stirred for 5 min. The volatiles were evaporated, and the residue was recrystallized in C_6H_5F layered with pentane. Yield: 190 mg (92%). ^1H NMR (C_6H_5F:C_6D_{12} = 10:1, 20 °C, 400 MHz): 4.09 (t, J_{HH} = 7.7 Hz, 2H, CH_2O), 3.04 (s, 3H, OCH_3), 2.07 (tt, J_{HH} = J_{PH} = 7.7 Hz, Ru−CH_2), 1.13 (vt, N = 13.7 Hz, 18H, PC(CH_3)$_3$), 1.09 (vt, N = 5.0 Hz, 6H, PCH_3), 0.90 (vt, N = 13.0 Hz, 18H, PC(CH_3)$_3$). $^{31}P\{^1H\}$ NMR (162 MHz): 45.0 (s). $^{13}C\{^1H\}$ NMR (100 MHz): 205.4 (t, J_{PC} = 15 Hz, Ru−CO), 89.6 (s, CH_2O), 60.6 (s, OCH_3), 38.0 (vt, N = 18 P*C*(CH_3)$_3$), 36.6 (vt, N = 18 P*C*(CH_3)$_3$), 29.3 and 29.0 (s, PC(*C*H_3)$_3$), 2.9 (vt, N = 17.4 Hz, PCH_3), −1.18 (t, J_{PC} = 5.5 Hz, Ru−CH_2). IR (C_6H_5F): 1939 cm^{-1} (ν(CO)).

Structure Determination of [Ru(η^2-CH_2CH_2OMe)(CO)(P^tBu_2Me)$_2$]BAr′$_4$, 9. The single crystals were grown from a solvent mixture of fluorobenzene and pentane at −20 °C. A medium-sized crystal was chosen from the bulk sample and affixed to the tip of a glass fiber with the use of silicone grease under nitrogen atmosphere. The mounted sample was then transferred, under a stream of dry nitrogen, to the goniostat; at the goniostat the crystal was inserted directly into the instrument's cryogenic stream and cooled to −174 °C for characterization and data collection. A systematic search of a limited hemisphere of reciprocal space located a set of data with tetragonal symmetry and with systematic absences uniquely characteristic of space group $P4_12_12$. Subsequent solution and refinement confirmed this space group choice. Data were collected by the moving-crystal−moving-detector technique with fixed background counts at each extreme of the scan. Data were corrected for Lorentz and polarization effects, and equivalent data were averaged. The structure was solved by direct methods (SHELXTL) and Fourier techniques. All hydrogen atoms were placed in calculated positions and refined with the use of a riding model. All non-hydrogen atoms except those representing the partially resolved solvent molecule were refined anisotropically. The structure solution and refinement were complicated by the fact that the entire cation is disordered about a 2-fold rotation axis. Even the ruthenium is slightly off axis. Especially problematic is that the disorder causes the images of the two phosphine ligands to be convoluted together. Successful refinement of the cation required that geometric restraints be applied to the phosphine ligands to influence them toward geometric consistency both internally and between the two ligands and also that thermal parameter restraints be applied to the atoms of those ligands. A final difference electron density map was featureless, with the largest peak having an intensity of 0.83 e/Å^3. The crystallographic data are collected in Table 1.

[Ru(η^2-$CH_2CH_2OC_2H_5$)(CO)(P^tBu_2Me)$_2$]BAr′$_4$. The same procedure as above was followed except using 1 equiv of CH_2=CH(OEt). ^1H NMR (C_6D_5F, 20 °C, 400 MHz): 3.81 (t, 2H, J_{HH} = 8 Hz, CH_2OEt), 3.14 (q, J_{HH} = 7.2 Hz, 2H, OCH_2Me), 1.88 (tt, J_{HH} = 8 Hz, J_{PH} = 8 Hz, 2H, Ru−CH_2), 1.00 (vt, N = 13.8 Hz, 18H, P^{t}Bu), 0.925 (vt, N = 4.8 Hz, 6H, PCH_3), 0.825 (t, J_{HH} = 7.2 Hz, 3H, CH_3), 0.763 (vt, N = 12.8 Hz, 18H, P^{t}Bu). $^{13}C\{^1H\}$ NMR (100 MHz, C_6D_5F, 20 °C): 205.4 (t, J_{PC} = 29 Hz, Ru−CO), 85.2 (s, CH_2O), 71.0 (s, OCH_2), 37.9 (vt, N = 19 Hz, P*C*Me$_3$), 36.7 (vt, N = 18 Hz, P*C*Me$_3$), 29.2 (s, PC(*C*H_3)$_3$), 29.0 (s, PC(*C*H_3)$_3$), 13.2 (s, OCH_2CH_3), 3.4 (vt, N = 17 Hz, PCH_3), −0.7 (t, J_{PC} = 5.5 Hz, Ru−CH_2). $^{31}P\{^1H\}$ NMR (162 MHz, 20 °C): 42.2 (s).

Low-Temperature Reaction of [RuH(CO)L_2]BAr′$_4$ with CH_2=CH(OEt). [RuH(CO)(P^tBu_2Me)$_2$]BAr′$_4$ (26 mg, 0.02 mmol) was dissolved in CD_2Cl_2 (0.5 mL) in an NMR tube with a Teflon screw cap. To the cold (−80 °C) wall of the tube was added CH_2=CH(OEt) (2.0 μL, 0.02 mmol); this was mixed thoroughly with the cold CD_2Cl_2 solution before the tube was transported to the −80 °C NMR probe for observation. After 30 min, most of the [RuH(CO)(P^tBu_2Me)$_2$]BAr′$_4$ was consumed to give [RuH(O(Et)(C_2H_3))(CO)(P^tBu_2Me)$_2$]BAr′$_4$. $^{13}P\{^1H\}$ NMR (162 MHz): 46.6 (d, J_{PP} = 224 Hz), 48.6 (d, J_{PP} = 224 Hz). ^1H NMR (400 MHz); −28.0 (t, J_{PH} = 14 Hz, Ru−H), 7.32 (d, J_{HH} = 11 Hz, C*H*OEt), 4.3, 3.70 (m, CH_2=CHO), 3.92 (br, OCH_2). As the temperature is warmed to −60 °C, two new products formed. They are [Ru(η^2-CH_2CH_2OEt)(CO)L_2]BAr′$_4$ and [Ru(CH(OEt)(Me))(CO)L_2]BAr′$_4$ with integration of about 1:1. Spectroscopic data for the latter: $^{31}P\{^1H\}$ NMR (162 MHz, −70 °C): 44.9 (d, J_{PP} = 202 Hz), 44.0 (d, J_{PP} = 202 Hz). ^1H NMR (−70 °C, 400 MHz): 5.5 (m, Ru−C*H*(OEt), 3.55, 3.37 (apparent quintet, J_{HH} = 8 Hz, diastereotopic OCH_2Me), 0.36 (s, β-agostic CH(OEt)CH_3). Upon warming to −40 °C, only [Ru(η^2-CH_2CH_2-OEt)(CO)L_2]BAr′$_4$ is detected.

Reaction of [RuH(CO)L_2]BAr′$_4$ with 2,3-Dihydrofuran. RuH(OTf)(CO)(P^tBu_2Me)$_2$ (100 mg, 0.16 mmol) and NaBAr′$_4$ (150 mg, 0.17 mmol) were mixed in C_6H_5F (1 mL) and vigorously stirred for 5 min. The solution was then centrifuged, and the liquid was transferred to an NMR tube. To the solution was syringed 2,3-dihydrofuran (10 mL, 0.17 mmol) to yield a bright yellow solution. After 1 h of mixing, the reaction is

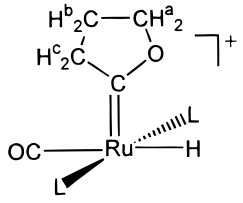

10

complete to give **10** in 90% yield based on $^{31}P\{^1H\}$ NMR integration. ^1H NMR (400 MHz, −10 °C): −1.71 (t, J_{PH} = 20 Hz, 1H, Ru−H), 0.87 (vt, N = 13.7, 18H, PC(CH_3)$_3$), 0.94 (vt, N = 13.8, 18H, PC(CH_3)$_3$), 1.30 (vt, N = 5 Hz, 6H, PCH_3), 1.50 (apparent quintet, J = 8 Hz, 2H, H^b), 2.84 (t, J_{HH} = 8 Hz, 2H, H^c), 4.0 (t, J_{HH} = 8 Hz, 2H, H^a), 7.75 (s, 4H, *para*-H of Ar′), 8.32 (s, 8H, *ortho*-H of Ar′). $^{31}P\{^1H\}$ NMR (162 Hz, −10 °C): 57.2 (s). $^{13}C\{^1H\}$ NMR (−10 °C): 302 (t, J_{PC} = 7 Hz, Ru=C), 201.5 (dt, J_{CH} = 35 Hz, from ^1H coupled ^{13}C spectrum, J_{PC} = 8 Hz), 82.7, 57.4, 23.6 (s, CH_2 of furan ring), 37.3 (vt, N = 21 Hz, P*C*Me$_3$), 36.8 (vt, N = 20 Hz, P*C*Me$_3$), 28.3 (s, PC(CH_3)$_3$), 27.9 (s, PC(CH_3)$_3$, 10.2 (vt, N = 24.4 Hz, PCH_3). After the NMR measurement, the solution was transferred to a test tube and layered with pentane for 24 h to give yellow crystals, which were filtered, washed with pentane, and dried to yield 120 mg (54%) product.

Acknowledgment. This work was supported by the National Science Foundation, the Université of Montpellier 2, and the French CNRS.

Supporting Information Available: Full crystallographic details, positional and thermal parameters, and distances and angles for **1**, **2**, **3**, and **9**. This material is available free of charge via the Internet at http://pubs.acs.org.

OM9910017